

DOI: 10.24425/amm.2021.134755

M. GUCWA^{1*}, J. WINCZEK¹, P. WIECZOREK², M. MIČIAN³, R. KOŃÁR³

THE ANALYSIS OF FILLER MATERIAL EFFECT ON PROPERTIES OF EXCAVATOR CRAWLER TRACK SHOE AFTER WELDING REGENERATION

The application of hardfacing is one of the ways to restore the functional properties of worn elements. The possibility of using filler materials rich in chrome allows for better wear resistance than base materials used so far. The paper presents the results of research on the use of 3 different grades of covered electrodes for the regeneration of worn track staves. The content of the carbon in the covered electrodes was from 0,5% to 7% and the chromium from 5% to 33%. The microscopic and hardness tests revealed large differences in the structure and properties of the welds. The differences in the hardness of the welds between the materials used were up to 150 HV units. The difference in wear resistance, in the ASTM G65 test, between the best and worst materials was almost 12 times big.

Keywords: hardfacing, carbides, hardness, wear, covered electrode

1. Introduction

The use of welding methods of regeneration is one of popular ways of restoring the usable properties of worn parts of machines and devices. Welding techniques allow to obtain properties in reconditioned elements as before wear or can significantly improve them. The undoubted advantage of using these techniques is a wide range of consumables that can be used during regeneration and in most cases moderate costs of surfacing operations. The process of regeneration can be done even in wet welding conditions [1,2]. A wide spectrum of filler materials for surfacing allows to obtain layers of chemical composition of non-alloy and alloy steels and cast irons with a high content of different types of carbides [3-6]. They also enrich surface in ceramics intermetallic phases [7-10] or deposit nanocrystalline materials [11, 12]. It is also possible to introduce carbide particles of a certain size into the surface layer [13]. Extensive research [14] shows that one of the most important factors determining the resistance of surfacing layers to wear is not the hardness but the chemical composition including carbon content in the material used. Carbides obtained in padded layers differ in their chemical composition, morphology and orientation in structure [15-17]. M_7C_3 type carbides are the most common carbides

found in hardfacing layers with high chromium content, which are characterized by high hardness and wear resistance as well as different morphology [15,18-19]. The chemical composition of M_7C_3 type carbides can be enriched by the addition of e.g. vanadium [20] or cerium [21,22], which affects structure fragmentation and increase in hardness. Also, the presence of titanium [23] and niobium [24] carbides positively increases the wear resistance in layers with a high content of M_7C_3 carbides. Due to the diverse work environment, the chemical composition should be selected depending on the anticipated wear model, e.g. metal-metal or metal-mineral. Obtaining appropriate properties in the surface layer, however, is associated with the correct selection of technological parameters of the surfacing process, so as to eliminate or reduce possible defects, e.g. cracks in the case of hard welds, and to obtain the appropriate structure of the surface layer for a specific application. This is particularly important for those applications where the potential consumption is intensive and may cause interruptions in the production process. One of such cases is the mining industry, in which welding methods of regeneration are eagerly used for e.g. elements of transport systems, excavator buckets or track elements.

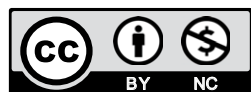
The present research work has the main goal in examinations of microstructure properties on the abrasion behaviour

¹ CZESTOCHOWA UNIVERSITY OF TECHNOLOGY, FACULTY OF MECHANICAL ENGINEERING AND COMPUTER SCIENCE, DĄBROWSKIEGO 69, 42-201 CZĘSTOCHOWA, POLAND

² CZESTOCHOWA UNIVERSITY OF TECHNOLOGY, FACULTY OF PRODUCTION ENGINEERING AND MATERIALS TECHNOLOGY, DĄBROWSKIEGO 69, 42-201 CZĘSTOCHOWA, POLAND

³ UNIVERSITY OF ŽILINA, DEPARTMENT OF TECHNOLOGICAL ENGINEERING, UNIVERZITNÁ 1, 010 26 ŽILINA, SLOVAKIA

* Corresponding author: mgucwa@spaw.pcz.pl



of 3 grades of hardfacing alloys, with different chemical composition, that could be applied on track shoe.

2. Experimental procedure

The subject of the study were bulldozer track shoe, which were naturally worn and were intended for regeneration. The chemical composition of the caterpillar material is shown in Table 1. Three grades of covered electrodes with the chemical compositions shown in Table 2 were selected for the hardfacing tests. The hardfacing was performed using the EWM Phoenix Plus welding machine. Surfacing tests for each of the electrodes were carried out with the parameters given in Table 3 and the heat input was calculated with coefficient $k = 0.8$. The three layers of welding, for each type of electrode, were carried out while maintaining the interpass temperature at 180°C. The prepared welds were then cut into samples for metallographic and wear resistance tests in accordance with ASTM G65. Prior to the test on the G65 tester, the test surfaces were grounded to ensure the best contact between the test sample and the wheel between which the abrasive in the form of silicon sand was fed with a flow rate of about 300 grams per minute. The test duration was 30 minutes (procedure A). Before the start of the test, the samples were weighed to the nearest 0.001 g and weighed again after the end of the test.

TABLE 1

Chemical composition of base material

Chemical composition of base material, % weight											
C	Si	Mn	P	S	Cr	Mo	Ni	Al	Co	Cu	Fe
0.20	0.3	1.4	0.06	0.03	0.38	0.04	0.17	0.05	0.01	0.13	Balance

TABLE 2

Chemical composition of deposited materials

Designation of samples	Chemical composition of deposited materials, % weight			
	C	Cr	Nb	Fe
A	7	22	7	Balance
B	3.3	32	—	Balance
C	0.5	5	—	Balance

TABLE 3

Hardfacing process parameters

Designation of samples	Diameter of the electrode mm	Welding current A	Arc voltage V	Heat input kJ/mm
A	5	252	29.7	1.79
B	3.2	131	25.2	0.79
C	3.2	131	25.2	0.79

The specimens used for metallography were subsequently etched with etching reagent (10 g CuCl₂, 10 ml HCl, 80 ml C₂H₅OH). Microstructure was observed with metallographic

light microscope Olympus GX51 and SEM JEOL JSM-6610. Hardness measurements were carried out with a standard Vickers hardness technique HV10 for macroscopic hardness.

3. Results and discussion

The width of hardfacings was 25 mm for each sample and the height was from 5 to 7 mm with depth of penetration from 0.8 to 1.7 mm. There were visible cracks in the perpendicular direction to the welding on samples A and B. The structure and properties of the obtained hardfacings show significant differences mainly due to the chemical composition of the electrodes used. Structure research focused mainly on the area near the hardfacing surface. It should be noted that the structure over the entire section of the welds was not homogeneous. The most homogeneous structure could be observed for sample A and C. In sample B, the structure changed strongly with the distance from the surface. In the case of material A and B, there are materials with a structure of chromium cast iron, while for layers welded with material C, it is a structure of alloy steels. In samples A (Fig. 1,2) and B (Fig. 3,4), numerous precipitations of large primary carbides and fine secondary eutectic carbides can be observed. In the case of the C-sample deposit, carbide precipitations are few and located along the martensite and bainite grain boundaries (Fig. 5,6). The morphology of carbide precipitations was strongly dependent on the distance from the surface. Near the surface, numerous spindle-shaped carbides, crystallizing in the direction of heat dissipation [25], and hexagonal-shaped carbides were observed. At a distance greater than 2 mm from the surface, numerous changes in the size and morphology of carbide precipitations could be observed for samples marked A and B. In the deeper layers of welds the number of primary carbides with a spindle-shaped shape was limited. This applies especially to the B weld, in which a strong fragmentation of carbides below the bonding area of the successive layers of the weld can be observed. For deposit A, the changes in the size of the carbide precipitation morphology are smaller. Grinding of primary carbides is observed, but large coniferous precipitation of primary carbides can still be observed even near the fusion line. These differences result from the amount of heat input and the crystallization conditions of welds thus induced [26-28]. Despite much higher heat input for welding A, its influence on the structure is smaller than in the case of welding B. It is necessary to take into account the volume of material that must be melted in a unit of time for electrodes with a diameter of 5 and 3.2 mm. For an electrode with a diameter of 3.2 mm, the amount of heat per 1 mm³ of the volume of the electrode to melt is greater in the experimental conditions than for an electrode with a diameter of 5 mm. The structure of the C-weld deposit is, as mentioned above, the most uniform, in which the top layer is dominated by martensite, while in the lower layers of the deposit, in addition to martensite, the structures of the lower bainite can be observed.

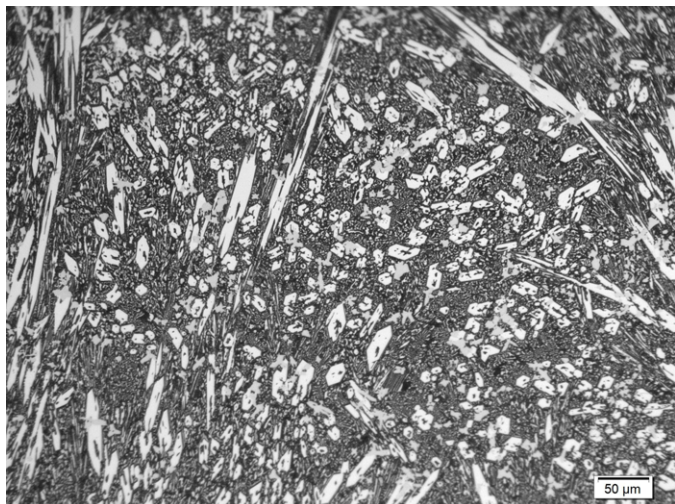


Fig. 1. Microstructure of sample A

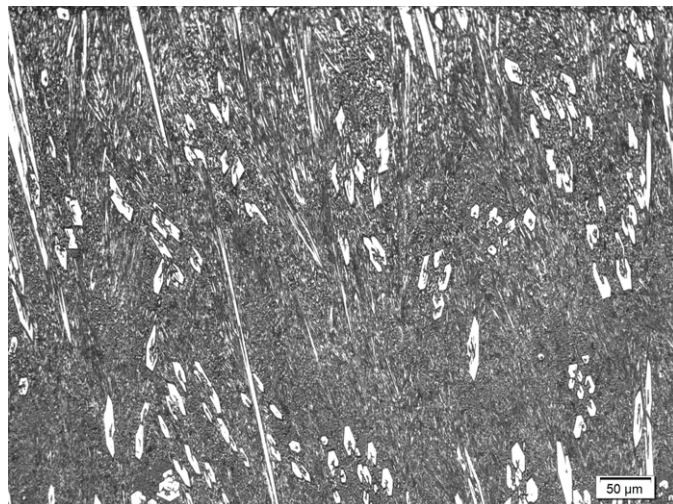


Fig. 3. Microstructure of sample B

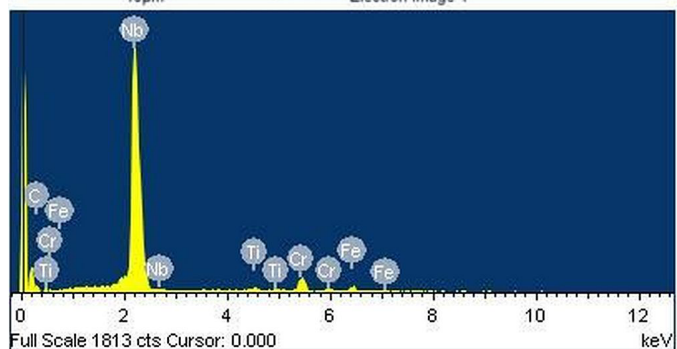
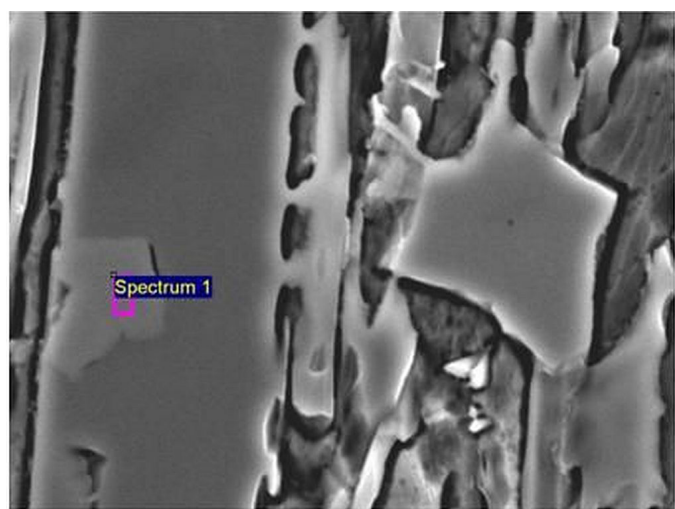


Fig. 2. SEM structure of sample A with Nb carbide inside chromium carbide

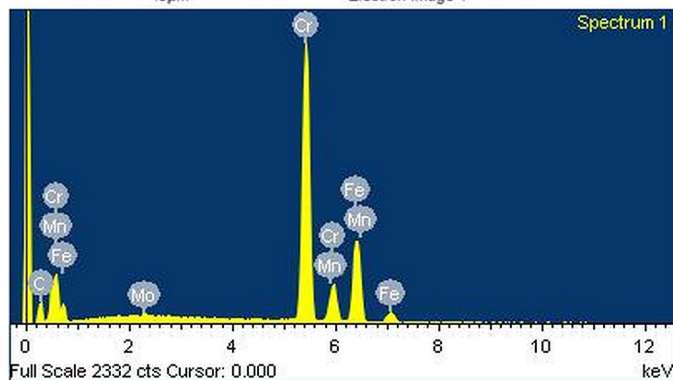
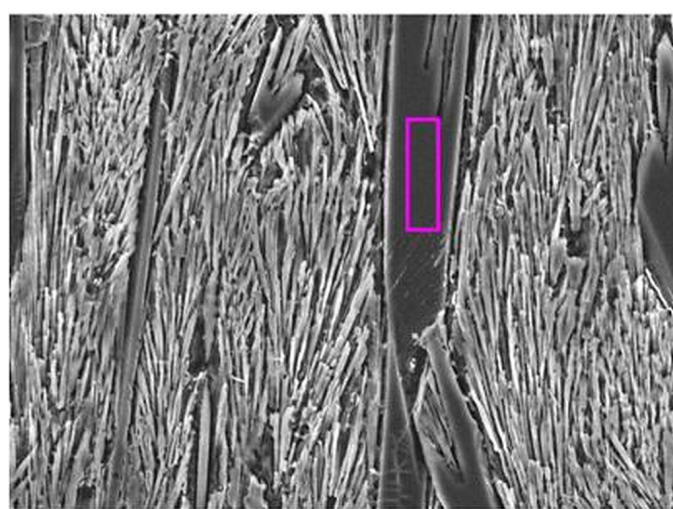


Fig. 4. SEM structure of sample B with chromium carbides

The hardness tests were carried out with 5 measurement points on the surface and Fig. 7 shows the average values of the tests. The hardness tests on the hardfacing surface (Fig. 7) confirmed the high hardness, which in the case of surfacing A was close to 800HV10. The difference in hardness on the tested surface in the case of samples B and C is only about 60 HV10 units despite the decidedly different structure of these materials. Despite the relatively small differences in the hardness of the

B and C materials tested, their wear resistance is definitely different. Figure 8 shows the results of hardness test on the cross section. The tests were carried out starting with 1.5 mm below the surface and continuing measurements approximately every 0.5 mm. The hardness in the HAZ for the tested samples ranged from 230 to 270 HV10. The hardness results in cross section confirmed the differences between the hardfacings and non homogenous character of the structure of each deposition. The

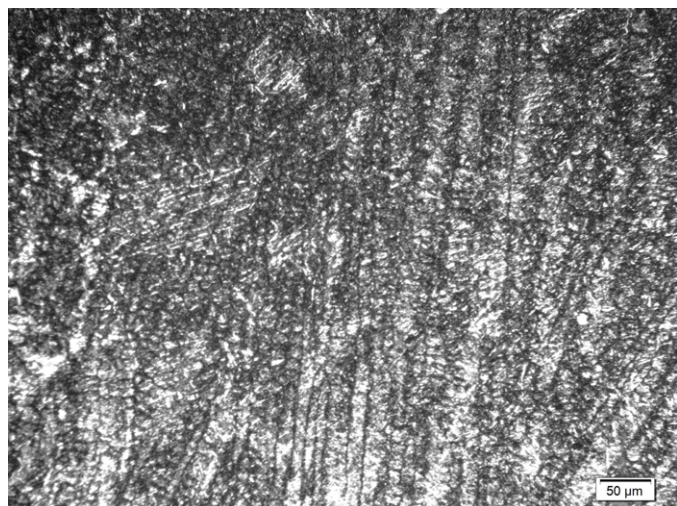


Fig. 5. Microstructure of sample C

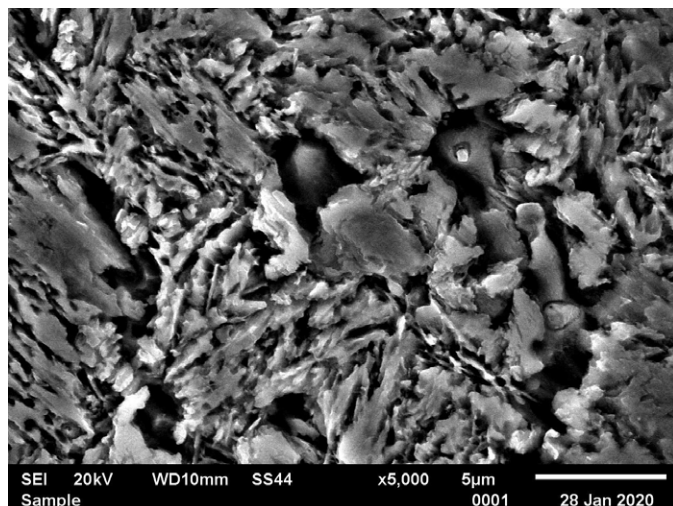


Fig. 6. SEM structure of sample C with chromium carbides located on the grains boundary

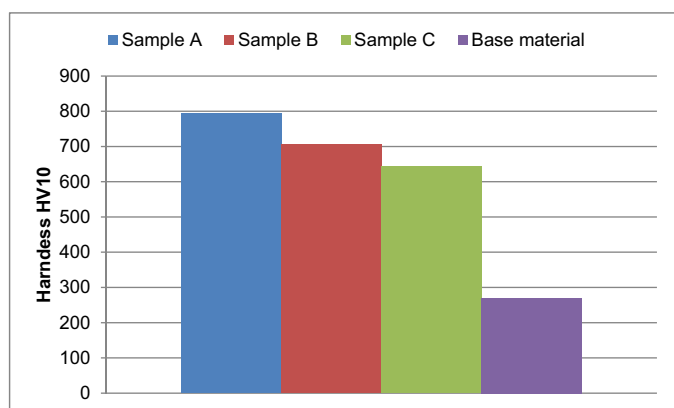


Fig. 7. The average hardness on the surfaces of the tested materials

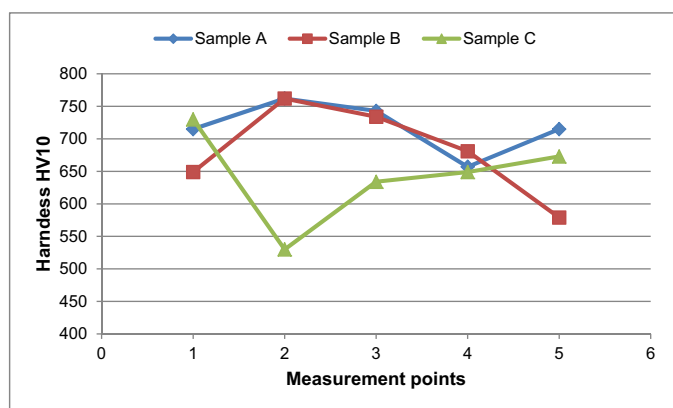


Fig. 8. The hardness in the cross section of the hardfacing materials

results of many studies indicate the decisive role of the structure and not the hardness in wear resistance [14,23,29].

The results presented in Table 4 indicate 5 times greater wear resistance of the sample B than of sample C. The best wear resistance was in sample A, which compared to the sample B had more than 2 times higher wear resistance in the test.

The remaining welds have cracks on their surface (Fig. 9 and 10), which are characteristic for welds with a high carbide content in the structure and high hardness. These cracks can, under unfavorable conditions, lead to a sharp decrease in wear resistance

TABLE 4

Results of the wear tests

Designation of the samples	Mass of the sample g		Mass loss g	Volume loss mm ³
	Before the test	After the test		
A	231.267	231.249	0.018	2.290
B	213.507	213.467	0.04	5.089
C	196.004	195.791	0.213	27.099
Base material	189.516	189.315	0.201	25.572

Tests of the wear resistance of the basic material showed that it has nearly 5% better wear resistance than the C weld. However, these values are similar to each other and it can be assumed that the C weld guarantees wear resistance at the base material level. Importantly, the C weld does not show surface cracks (Fig. 11).

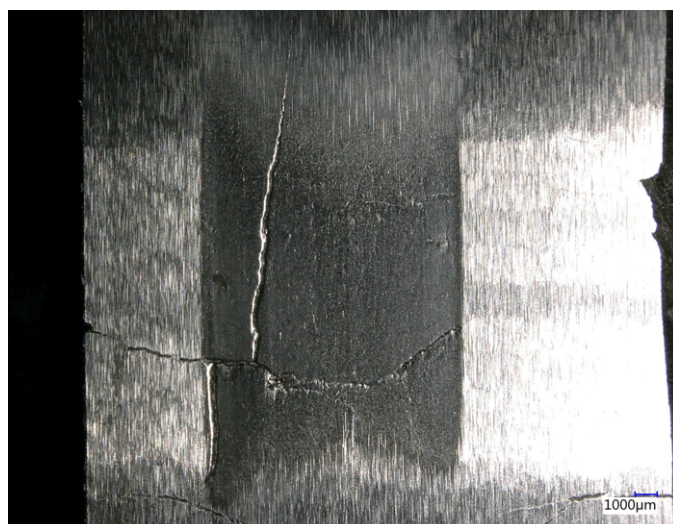


Fig. 9. The surface of the sample A after wear test

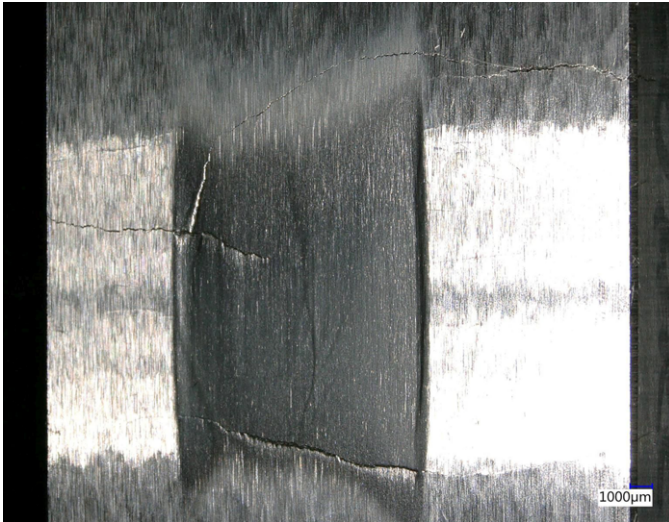


Fig. 10. The surface of the sample B after wear test

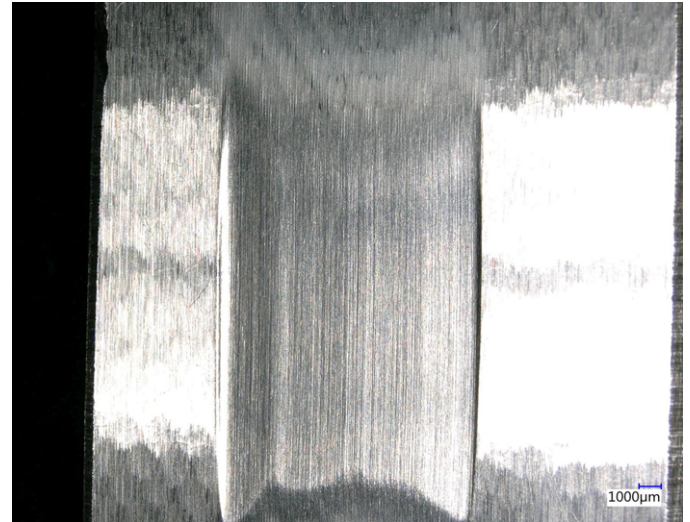


Fig. 11. The surface of the sample C after wear test

by bonding large fragments of the deposit. Pre-heating before welding can reduce the number of cracks occurring, however, it can also lead to a decrease in wear resistance [30]. The change in hardness on the cross-section of the welds (Fig. 8) is the result of the heat welding cycles and the overlap of successive layers of welds. In the case of surfacing A, large primary carbides of spindle and hexagonal shape and hardness occur in almost the entire cross-section, which guarantee good wear resistance. Large primary carbides provide some protection for eutectic carbide colonies against abrasive particles [31]. Their arrangement in relation to the direction of the abrasive is important. Tests [15] showed greater wear resistance of M_7C_3 carbides in the case of carbides located in the transverse direction to the surface. Also, the presence of niobium carbides increases wear resistance in the A deposit and their accidental orientation in structure [24]. For sample C, larger changes in the hardness and size of carbide precipitations can be observed, which can translate into greater material consumption during operation. As already mentioned, sample C has the most uniform structure, however, hardness tests showed the existence of areas with reduced hardness, in which the lower bainite dominates, what may increase the wear. In addition, a very small number of finely dispersive carbides (Fig. 6) are not a sufficient barrier to wear factors.

4. Conclusions

- The best wear resistance in the experiment was for the sample A with higher content of carbon and chromium. The structure of this hardfacing was rich in big spindle shaped and hexagonal shaped carbides in the whole cross section. It is a guarantee of similar wear resistance in whole volume of the layer.
- In the hardfacing with structure of the cast iron (sample A and B) there are numbers of cracks on the surface. Despite the presence of the cracks the results of the wear test were close to 12 times better than to the base material without

the cracks. The potential problem is in the role of cracks in the severe wear condition in which the visible cracks could be the cause of the rapid increase of the wear by the removing of the large volume of the materials.

- The results of the wear in the base material and sample C is almost the same despite the significant difference in the hardness. The structure of the sample C almost without the carbides and martensite-bainite structure is susceptible on the wear with abrasive particles. The main advantage of this material is the lack of crack and similar wear resistance as the base material.

REFERENCES

- [1] J. Tomków, D. Fydrych, G. Rogalski, *Materials* **12** (20), 3372 (2019), DOI:10.3390/ma12203372.
- [2] J. Tomków, A. Czupryński, D. Fydrych, *Coatings* **10**, 219 (2020) DOI:10.3390/coatings10030219.
- [3] A. Zikin, I. Hussainova, C. Katsich, E. Badisch, C. Tomastik, *Surf. Coat. Technol.* **206**, 4270-4278 (2012), DOI:10.1016/j.surfcoat.2012.04.039.
- [4] M. Kirchgaßner, E. Badisch, F. Franek, *Wear*. **265**, 772-779 (2008), DOI:10.1016/j.wear.2008.01.004.
- [5] C.M. Lin, H.H. Lai, J.C. Kuo, W. Wu, *Mater. Charact.* **62**, 1124-1133 (2011), DOI:10.1016/j.matchar.2011.09.007.
- [6] X.H. Wang, F. Han, X.M. Liu, S.Y. Qu, Z.D. Zou, *Mater. Sci. Eng. A*. **489**, 193-200 (2008), DOI:10.1016/j.msea.2007.12.020.
- [7] M. Szala, L. Łatka, M. Walczak, M. Winnicki, *Metals* **10** (7), 856 (2020), DOI:10.3390/met10070856.
- [8] T. Chmielewski, P. Siwek, M. Chmielewski, A. Piątkowska, A. Grabias, D. Golański, *Metals* **8** (12), 1059 (2018), DOI:10.3390/met8121.
- [9] M. Adamiak, A. Czupryński, A. Kopyś, Z. Monica, M. Olender, A. Gwiazda, *Metals* **8**, 142 (2018), DOI:10.3390/met8020142.
- [10] A. Czupryński, J. Górka, M. Adamiak, B. Tomiczek, *Arch. Metall. Mater.* **61**, 1363-1370 (2016), DOI:10.1515/amm-2016-0224.

- [11] J. Górka, A. Czupryński, M. Żuk, M. Adamiak, A. Kopyś, *Materials* **11**, 1184 (2018), DOI:10.3390/ma11071184.
- [12] J. Górka, *J. Min. Metall. Sect. B-Metall.* DOI: 10.2298/accepted_manuscript (pdf).
- [13] V. Jankauskas, M. Antonov, V. Varnauskas, Re. Skirkus, D. Goljandin, *Wear*. **328-329**, 378-390 (2015), DOI:10.1016/j.wear.2015.02.063.
- [14] D.J. Kotecki, J.S. Ogborn, *Weld. J.* **74** (8), 269-278 (1995).
- [15] J.J. Coronado, *Wear*. **270**, 287-293 (2011), DOI:10.1016/j.wear.2010.10.070.
- [16] H.H. Lai, C.C. Hsieh, C.M. Lin, W. Wu, *Surf. Coat. Technol.* **239**, 233-239 (2014), DOI: 10.1016/j.surfcoat.2013.11.048.
- [17] Y. Lv, Y. Sun, J. Zhao, G. Yu, J. Shen, S. Hu, *Mater. Des.* **39**, 303-308 (2012), DOI: 10.1016/j.matdes.2012.02.048.
- [18] S.D. Carpenter, D.E.O.S. Carpenter, J.T.H. Pearcec, *J. Alloys Compd.* **494**, 245-251 (2010), DOI:10.1016/j.jallcom.2009.12.197.
- [19] S. Liu, Y. Zhou, X. Xing, J. Wang, X. Ren, Q. Yang, *Sci. Rep.* **32941**, 1-8(2016), DOI: 10.1038/srep32941.
- [20] X. Qi, Z. Jia, Q. Yang, Y. Yang, *Surf. Coat. Technol.* **205**, 5510-5514 (2011), DOI:10.1016/j.surfcoat.2011.06.027.
- [21] Y.F. Zhou, Y.L. Yang, Y.W. Jiang, J. Yang, X.J. Ren, Q.X. Yang, *Mater. Charact.* **72**, 77-86 (2012), DOI:10.1016/j.matchar.2012.07.004.
- [22] S. Xing, S. Yu, Y. Deng, M. Dai, L. Yu, *Journal of Rare Earths* **30**, 69-73(2012), DOI: 10.1016/S1002-0721(10)60641-2.
- [23] J.J. Coronado, H.F. Caicedo, A.L. Gómez, *Tribol. Int.* **42**, 745-749 (2009), doi:10.1016/j.triboint.2008.10.012.
- [24] M.F. Buchely, J.C. Gutierrez, L.M. León, A. Toro, *Wear* **259**, 52-61 (2005), doi:10.1016/j.wear.2005.03.002.
- [25] E.O. Correa, N.G. Alcântara, L.C. Valeriano, N.D. Barbedo, R.R. Chaves, *Surf. Coat. Technol.* **276**, 479-484 (2015), DOI: 10.1016/j.surfcoat.2015.06.026.
- [26] N.G. Chaidemenopoulos, P.P. Psyllaki, E. Pavlidou, G. Vourlias, *Surf. Coat. Technol.* **357**, 651-661 (2019), DOI:10.1016/j.surfcoat.2018.10.061.
- [27] S. Pawara, A.K. Jha, G. Mukhopadhyay, *Int. J. Refract. Met. H.* **78**, 288-295 (2019), DOI:10.1016/j.ijrmhm.2018.10.014.
- [28] C.M. Chang, C.M. Lin, C.C. Hsieh, J.H. Chen, C.M. Fan, W. Wu, *Mater. Chem. Phys.* **117**, 257-261 (2009), DOI:10.1016/j.matchemphys.2009.05.052.
- [29] S. Chatterjee, T.K. Pal, *Wear* **255**, 417-425 (2003), DOI:10.1016/S0043-1648(03)00101-7.
- [30] M. Gucwa, J. Winczek, M. Mician, *Weld. Tech. Rev.* **92** (2), 7-14 (2020), DOI:10.26628/wtr.v92i2.1096.
- [31] C.M. Chang, Y.C. Chen, W. Wu, *Tribol. Int.* **43**, 929-934 (2010), DOI:10.1016/j.triboint.2009.12.045.